

E. coli Histidine Triad Nucleotide Binding Protein 1 (ecHinT) Is a Catalytic Regulator of D-Alanine Dehydrogenase (DadA) Activity *In Vivo*

Sanaa Bardaweel¹, Brahma Ghosh¹, Tsui-Fen Chou¹, Michael J. Sadowsky^{2*}, Carston R. Wagner^{1*}

¹ Department of Medicinal Chemistry, University of Minnesota, Minneapolis, Minnesota, United States of America, ² Department of Soil, Water and Climate and the Biotechnology Institute, University of Minnesota, St. Paul, Minnesota, United States of America

Abstract

Histidine triad nucleotide binding proteins (Hints) are highly conserved members of the histidine triad (HIT) protein superfamily. Hints comprise the most ancient branch of this superfamily and can be found in Archaea, Bacteria, and Eukaryota. Prokaryotic genomes, including a wide diversity of both Gram-negative and Gram-positive bacteria, typically have one Hint gene encoded by *hinT* (*ycfF* in *E. coli*). Despite their ubiquity, the foundational reason for the wide-spread conservation of Hints across all kingdoms of life remains a mystery. In this study, we used a combination of phenotypic screening and complementation analyses with wild-type and *hinT* knock-out *Escherichia coli* strains to show that catalytically active ecHinT is required in *E. coli* for growth on D-alanine as a sole carbon source. We demonstrate that the expression of catalytically active ecHinT is essential for the activity of the enzyme D-alanine dehydrogenase (DadA) (equivalent to D-amino acid oxidase in eukaryotes), a necessary component of the D-alanine catabolic pathway. Site-directed mutagenesis studies revealed that catalytically active C-terminal mutants of ecHinT are unable to activate DadA activity. In addition, we have designed and synthesized the first cell-permeable inhibitor of ecHinT and demonstrated that the wild-type *E. coli* treated with the inhibitor exhibited the same phenotype observed for the *hinT* knock-out strain. These results reveal that the catalytic activity and structure of ecHinT is essential for DadA function and therefore alanine metabolism in *E. coli*. Moreover, they provide the first biochemical evidence linking the catalytic activity of this ubiquitous protein to the biological function of Hints in *Escherichia coli*.

Citation: Bardaweel S, Ghosh B, Chou T-F, Sadowsky MJ, Wagner CR (2011) *E. coli* Histidine Triad Nucleotide Binding Protein 1 (ecHinT) Is a Catalytic Regulator of D-Alanine Dehydrogenase (DadA) Activity *In Vivo*. PLoS ONE 6(7): e20897. doi:10.1371/journal.pone.0020897

Editor: Michael Polymenis, Texas A&M University, United States of America

Received: March 11, 2011; **Accepted:** May 11, 2011; **Published:** July 6, 2011

Copyright: © 2011 Bardaweel et al. This is an open-access article distributed under the terms of the Creative Commons Attribution License, which permits unrestricted use, distribution, and reproduction in any medium, provided the original author and source are credited.

Funding: Funding was provided by the University of Minnesota. No external funding sources for this study. The funders had no role in study design, data collection and analysis, decision to publish, or preparation of the manuscript.

Competing Interests: The authors have declared that no competing interests exist.

* E-mail: wagne003@umn.edu (CRW); sadowsky@umn.edu (MJS)

Introduction

Histidine triad nucleotide binding proteins (Hints) are conserved from bacteria to humans [1]. While prokaryotes typically encode only one Hint gene, eukaryotes generally contain two to three different Hint genes [2]. The physiological role of Hints in mammalian cells is just now being delineated. Two hybrid screening experiments revealed that Hint1 interacts with Cdk7, the catalytic subunit of the cyclin dependent kinase activation complex Cdk7-cyclin H-MAT1 [3]. However, Hint1 mouse knock-out studies indicated that Hint1 is not required for Cdk7 function [4]. The human Hint1 (hHint1) has also been shown to directly interact with human Pontin and Reptin in the TCF- β -catenin transcription complex [5]. It has been reported that hHint1 might be a tumor suppressor [6,7]. Like other tumor suppressor proteins, Hint1 is associated with pro-apoptotic properties [8]. More recently, human Hint1 (hHint1) has been reported to participate in the development of hepatic ischemia reperfusion injury [9]. In addition, recent studies have shown that hHint1 is involved in the regulation of postsynaptic dopamine transmission [10]. Recently, we reported that hHint1 and *E. coli* Hint (ecHinT) hydrolyze lysine-AMP generated by bacterial and human LysRS, suggesting that Hints have a specific role in regulating LysRS [11].

E. coli Hint (encoded by *hinT*) has high sequence similarity to hHint1 (ecHinT is 48% identical to hHint1 at the amino acid level) and has been shown to form stable potential protein-protein interactions with six proteins: a putative oxidoreductase and formate dehydrogenase (b1501), the heat shock protein 70 (Hsp70), the β -subunit of DNA polymerase III (*dnaN*), a membrane-bound lytic murein transglycosylase D (*dnr*), ET-Tu elongation factor (*tufA*), and a putative synthetase (*yjhH*) [12]. In addition, the HinT from *Mycoplasma* has been shown to interact with two membrane proteins (P60 and P80) [13,14]. With regard to the importance of Hint1 catalytic activity, yeast strains constructed with a catalytically deficient mutant of the ortholog, Hnt1, failed to grow on galactose at elevated temperatures, suggesting that the catalytic activity of Hnt1 is required for the phenotype [15]. Nevertheless, the physiological and biochemical basis for the relationship of Hints to these interactions and associated phenotypes, as well as the foundational reason for their wide-spread conservation across all three kingdoms of life remains enigmatic.

Crystal structure studies of hHint1 and, recently, ecHinT have revealed that both proteins are homodimers containing an active-site with four conserved histidines [16,17]. While similar, close

inspection of the two structures revealed little sequence similarity between their C-termini. In contrast to hHint1, the longer C-terminus of ecHinT was found to adopt eight different conformations in the unit cell [17]. Chimeric domain swap mutants, in which the C-termini of both ecHinT and hHint1 have been switched, have demonstrated the importance of the C-termini on model substrate specificity [18]. Moreover, deletion mutagenesis studies have shown that the loss of just three C-terminal side-chains abolishes the ability of ecHinT to hydrolyze LysRS-generated lysine-AMP, while having only a modest effect on the catalytic efficiency of the enzyme with model substrates [17]. Although catalytic insights of Hint activity have been garnered from these studies, a defined biochemical rationale for the function of Hints in general, and ecHinT in particular, has remained elusive.

Phenotype characterization is an essential approach for understanding structure-function relationships among a variety of biological systems. While several advanced and comprehensive technologies have been developed to sequence and identify functions of genes and their products, and assign them to particular metabolic pathways, the function of many genes in most organisms that have been sequenced to date remains unknown. For example, although *E. coli* is considered to be amongst the most genetically characterized microorganisms, about 30–40% of its genes have unknown function [19]. In an effort to determine the function of many of these “unknown” genes, a library of single gene knock-out mutants of all nonessential *E. coli* K-12 genes has been generated [20]. The metabolic profiles of many of these knock-out mutants have been characterized using Phenotype MicroArrays (PM) that allow testing of a large number of cellular phenotypes in 96-well microplates [21]. Based on the same redox chemistry, BiologTM phenotypic screening plates have been developed as a simplified universal reporter of metabolism in a single bacterium.

Given the high sequence similarity between hHint1 and ecHinT, we hypothesized that determining the function of Hint in *E. coli* may reveal a conserved biochemical and physiological role for Hints in general. In *E. coli* K-12, *in silico* analysis indicates that *hinT* is located in an apparent operon consisting of the *hinT(ycfF)-ycfL-ycfM-ycfN(thiK)-ycfO(nagZ)-ycfP* genes. In the study reported here, we investigated the role of *hinT* in *E. coli* by carrying out BiologTM phenotypic metabolic analyses with single gene deletion mutants. In addition, we investigated the role of ecHinT catalysis and structure on the observed ecHinT phenotype with a combination of site-directed mutagenesis and chemical biological studies. Our results show that ecHinT catalytic activity and the C-terminal domain are required for *E. coli* to grow on D-alanine as a sole carbon and energy source by the regulation of D-amino acid dehydrogenase activity. Taken together, our results demonstrate that ecHinT plays an essential role in the regulation of the fate of alanine in cellular compartments and thus links for the first time the catalytic activity and structure of a Hint protein with a bacterial physiological function.

Methods

Bacterial strains, media, and growth conditions

The bacterial strains used in this study were obtained from the *E. coli* Genetic Stock Center at Yale University and are listed in Table S1. All strains were received as glycerol stocks on filters, sub-cultured twice on Luria–Bertani (LB) agar medium [22], and incubated at 37°C for 48 h before testing. Liquid cultures were grown aerobically in LB medium supplemented with kanamycin

(50 µg/ml) at 37°C, with shaking, for 18 h. Strains were stored as 10% glycerol stocks at –80°C.

PCR verification of mutants

The mutations in gene knock-out mutants were verified using the polymerase chain reaction (PCR) technique. Primers sequences for each PCR reaction are listed in Table S2. DNA from freshly isolated colonies served as templates for PCR and reactions were initiated following a “hot start” protocol at 95°C. The first PCR reaction was used to confirm the expected size of *hinT* operon with a single gene deletion and insertion of a *kan* resistance gene. The second PCR reaction confirmed the junction points of the *kan* resistance gene in each knock-out mutant. PCR conditions were as follows: 94°C for 2 min followed by 30 cycles of 94°C for 30 s, 55°C for 30 s, and 72°C for 2 min.

Verification of *hinT* deletion mutant by loss of activity

The turnover rates of the fluorogenic substrate tryptamine 5'-adenosine phosphoramidate (TpAd) by ecHinT protein in cell-free lysates of wild-type *E. coli* BW25113 and the *hinT* deletion mutant (Δ *hinT*) was determined using a previously described phosphoramidase assay [23]. The excitation wavelength was 280 nm and fluorescence emission was measured at 360 nm. All kinetic assays were performed in duplicate at 25°C. The substrate hydrolysis rate was determined by measuring fluorescence increase following addition of 5–10 µl of lysates (8 ng total protein).

Phenotype analysis using BiologTM GN2-MicroPlates

Phenotypic analyses of *hinT* operon mutants containing single gene deletions were determined using BiologTM GN2-MicroPlates (Biolog Inc., Hayward, CA). Mutants were inoculated onto R2A agar plates containing, per liter, 0.5 g casamine acids, 0.5 g of D-glucose, 0.3 g sodium pyruvate, 0.3 g K₂HPO₄, 0.05 g MgSO₄·7H₂O, 0.5 g proteose peptone, 0.5 g soluble starch, 0.5 g yeast extract, and 15 g agar and incubated overnight at 37°C. Cells were swabbed from the surface of the agar plate, suspended in GN/GP-IF inoculating fluid (Biolog Inc., Hayward, CA) to a final OD_{600 nm} of 0.7, and inoculated into the GN2-MicroPlate (150 µl per well). The microplates were incubated at 30°C for 24 h, and absorbance values at 540 nm and 630 nm were determined using an EL808 Ultra Microplate reader (Bio-Tek Instruments Inc., Winooski, VT).

Carbon source utilization assays

Overnight cultures of wild-type and mutant *E. coli* strains were grown at 37°C, with shaking at 200 rpm, in LB medium supplemented with kanamycin (50 µg/ml) as needed. Cell pellets were obtained by centrifugation at 6000 × g at 4°C for 10 min. Pellets were washed twice and re-suspended in minimal medium containing (per liter): 6.8 g Na₂HPO₄, 3.0 g KH₂PO₄, 0.5 g NaCl, 1.0 g NH₄Cl, 0.001 g CaCl₂, 0.001 g MgSO₄, and 0.004 g thiamine, (pH 7.0). Carbon sources, D,L-alanine, glycerol, or glucose, were added, after autoclaving the medium, to a final concentration of 20 mM when needed.

Induction of D-amino acid dehydrogenase activity and enzyme assays

Induction of D-amino acid dehydrogenase in wild-type and mutant strains was achieved by adding 100 mM D,L-alanine to minimal medium containing 10% (vol/vol) glycerol as the sole carbon source. Cultures were grown at 37°C for 24 h prior to collection of cell pellets. D-amino acid dehydrogenase activity was measured by following the reduction of 2,6-dichlorophenol-

indophenol (DCPIP) at 600 nm as previously described [24]. Reaction mixtures contained 50 mM potassium phosphate buffer (pH 7.0), 10 mM KCN, 0.5 mM phenazine methosulfate, 10 mM DCPIP, and 100 mM of D,L-alanine. The reduction of absorbance at 600 nm was measured for 5 min using Varian Cary 50 UV-visible spectrophotometer (Palo Alto, CA, USA). The amount of DCPIP reduced was determined using a molar extinction coefficient of 21,500. All assays were produced in triplicate, and rates were determined from the first 2 min of activity. Activity is expressed as nmoles DCPIP reduced/min/mg protein, and rates between replicates varied by <5%.

Preparation of membrane fractions

Wild-type and mutant strains were grown to late exponential phase ($OD_{600\text{ nm}} = 0.9\text{--}1.1$) in minimal medium containing 100 mM D,L-alanine and 10% (vol/vol) glycerol, harvested by centrifugation at 10,000× g, and washed once in 0.85% NaCl. The pellets were stored at -80°C . Cell pellets were thawed, suspended in MOPS Buffer (10 mM MOPS, (pH 7.5), 20 mM MgCl_2 , and 10% glycerol) and passed twice through a French Pressure Cell at 11,000 psi. Cell lysates were centrifuged for 10 min at 14,500× g and the resulting supernatant was centrifuged for 80 min at 37,000× g in a Beckman Ultracentrifuge. The membrane fractions were obtained as described previously [25]. Aliquots of membrane fractions were stored at -80°C and used only once after thawing.

Reverse transcription-PCR

Total RNA was isolated from *E. coli* strains using Qiagen RNeasy minikit (Qiagen, Valencia, CA) according to the manufacturer's protocols. RNA concentration was determined spectrophotometrically at 260 nm and RNA quality was confirmed by electrophoresis of 1 μg of total RNA from each preparation on a 1.2% denatured agarose gel. The following primers were used for RT-PCR analysis: LP 5'GTTTCGATAACCGCATTCGT3' and RP 5'CCGGTATTCAGCCACAGATT3'. The RT-PCR conditions were adapted from Qiagen OneStep RT-PCR Kit handbook and were as follows: 50°C for 30 min, 95°C for 15 min followed by 30 cycles of 94°C for 0.5 min, 50°C for 0.5 min, 72°C for 0.5 min followed by a single 10-min cycle at 72°C for extension.

Site-directed mutagenesis

All *hinT* mutants were generated from *E. coli hinT*-pSGA02, the expression vector harboring the gene encoding wild-type *hinT*, by using the Quick-Change mutagenesis kit (Stratagene, Santa Clara, CA) following the manufacturer's protocol. Mutagenesis of ecHinT and hHint1 to produce ec/Hs and Hs/ec chimeric proteins was described previously [18].

Phenotype complementation studies

The preparation of competent cells was achieved using a Z-Competent *E. coli* Transformation Kit and Buffer Set (Zymo Research Corporation, Orange, CA). The $\Delta hinT$ mutant was transformed with 20 ng of plasmid DNA encoding either the wild-type *hinT*, H101A, H101G, $\Delta 114\text{--}119$, $\Delta 117\text{--}119$, Hs/ec chimera or ec/Hs chimera. Cultures were grown in LB medium, induced with IPTG (500 μM) when the culture reached $OD_{600\text{ nm}} = 0.4\text{--}0.7$, and incubated for an additional 10 h. Cell pellets were obtained by centrifugation at 6000× g for 10 min at 4°C , washed twice in M9 minimal medium [22], and re-suspended in 200 μl of the same medium. A 10–20 μl aliquot of the cell suspension was inoculated into M9 medium supplemented with 20 mM

D,L-alanine or glucose, with ampicillin (100 $\mu\text{g}/\text{ml}$) and kanamycin (50 $\mu\text{g}/\text{ml}$), to an initial $OD_{600\text{ nm}} = 0.06\text{--}0.08$. Cells were incubated at 37°C and $OD_{600\text{ nm}}$ was measured after for 36–40 h of growth.

General synthetic procedures and materials

All reagents were purchased from commercial vendors and used without further purification. Anhydrous pyridine was used from previously unopened SureSeal or AcrosSeal bottles. Analytical thin layer chromatography (TLC) was performed on 0.25 mm pre-coated Merck silica gel (SiO_2) 60 F254. Column chromatography was performed on Purasil 60A silica gel, 230–400 mesh (Whatman). ^1H and ^{31}P NMR were recorded on a Varian Mercury-300 or a Varian MR 400 spectrometer. Chemical shifts are reported in ppm relative to residual dimethyl sulfoxide (DMSO-d_6) peak. High-resolution mass spectrometry (HRMS) data were obtained on a Biotof II (Bruker) ESI-MS spectrometer.

Synthesis of 2',3'-Isopropylidene-5'-O-(4-chlorophenoxy)carbonyl guanosine (Guanosine -5'-carbonate acetone, 1)

Guanosine-2',3'-acetone (0.231 mmol) was dissolved in anhydrous pyridine (7 ml) in a 2-neck round-bottomed flask equipped with an Ar. inlet and a microsyringe. The stirred solution was chilled over a dry ice-acetone bath and 4-chlorophenyl chloroformate (0.278 mmol, 1.20 eq) was added dropwise under Ar. The cooling bath was removed and the solution was slowly allowed to return to room temperature. Stirring was continued until thin layer chromatographic and ESI-MS analyses showed that all of the starting material had disappeared (after approximately 4 h). Pyridine was evaporated *in vacuo* by co-distillation with n-heptane and the crude solid obtained was purified by chromatography on SiO_2 gel to isolate the guanosine-5'-carbonate as a white solid with a 90% yield. The ^1H NMR spectrum was (DMSO-d_6): 1.30 (s, 3H, $-\text{CH}_3$), 1.56 (s, 3H, $-\text{CH}_3$), 4.28–4.58 (m, 3H, $\text{C}2'+\text{C}3'+\text{C}4'\text{-H}$), 5.22 (s, 2H, $5'\text{-CH}_2$), 6.22 (s, 1H, $\text{C}1'\text{-H}$), 6.58 (s, 2H, NH_2), 7.22 (d, 2H, $-\text{Ph}$), 7.50 (d, 2H, $-\text{Ph}$), 7.86 (s, 1H, $\text{C}8\text{-H}$), 10.74 (s, 1H, $\text{N}1\text{-H}$) ppm.

Synthesis of 2',3'-Isopropylidene-5'-O-[(3-indolyl)-1-ethyl]carbamoyl guanosine (Guanosine -5'-carbamate acetone, 2)

A mixture of guanosine-5'-carbonate (0.255 mmol) and tryptamine (0.640 mmol, 2.5 eq) in anhydrous THF (10 ml) was heated to 60°C (oil bath) under Ar. and stirred at that temperature until TLC showed complete consumption of the starting material (4 h). The solvent was removed by rotary evaporation and the residue chromatographed on SiO_2 gel using $\text{CH}_2\text{Cl}_2:\text{MeOH}:\text{H}_2\text{O}$ (5:2:0.25) to give the title carbamate as white amorphous solid (yield 90%). The ^1H NMR spectrum was (DMSO-d_6): 1.32 (s, 3H, $-\text{CH}_3$), 1.58 (s, 3H, $-\text{CH}_3$), 2.80 (t, 2H, $-\text{CH}_2-$), 3.24 (q, 2H, $-\text{CH}_2\text{NHCO}$ 4.00–4.30 (m, 3H, $5'\text{-CH}_2+\text{C}4'\text{-H}$), 5.10 (d, 1H, $5'\text{-C}3'\text{-H}$), 5.24 (d, 1H, $\text{C}2'\text{-H}$), 6.00 (s, 1H, $\text{C}1'\text{-H}$), 6.58 (s, 2H, NH_2), 6.96 (t, 1H, indole), 7.12 (t, 1H, $-\text{indole}$), 7.18 (s, 1H, indole), 7.36 (d, 1H, indole), 7.40 (t, 1H, $-\text{NH}$), 7.50 (d, 1H, indole), 7.84 (s, 1H, $\text{C}8\text{-H}$), 10.72 (s, 1H, $\text{N}1\text{-H}$), 10.82 (s, 1H, NH-indole) ppm.

Synthesis of 5'-O-[(3-indolyl)-1-ethyl]carbamoyl guanosine (Guanosine-5'- tryptamine carbamate, TpGc)

The above 2', 3'acetone-protected guanosine carbamate (100 mg) was dissolved in $\text{TFA}:\text{H}_2\text{O}$ (4:1, 5 ml) and stirred at room temperature until TLC and ESI-MS showed no starting

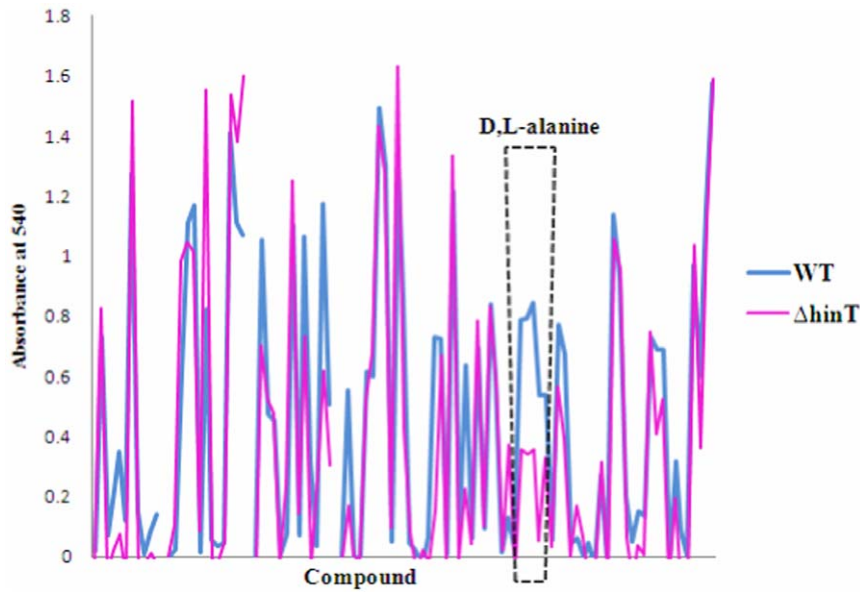


Figure 1. Summary of metabolic fingerprints. Dataset of the GN2 plate assay of wild-type *E. coli* BW25113 and $\Delta hinT$ mutant strains was processed as described in experimental procedures. The overlay represents the difference between the ability of the two strains to use 95 carbon sources. This is a representative overlay of three independent experiments. doi:10.1371/journal.pone.0020897.g001

material left (60 min). The mixture was stripped to dryness and the residue purified by SiO_2 gel chromatography using CH_2Cl_2 :
MeOH:H₂O (5:3:0.5) as eluant. The relevant UV-active fractions were collected and concentrated to afford the final compound as a white solid (yield 40%). The ¹H NMR spectrum was (DMSO-d₆): 2.38 (t, 2H, -CH₂-), 3.17 (q, 2H, -CH₂NHCO), 4.23–4.33 (m, 2H, 5'-CH₂), 4.56 (t, 1H, C4'-H), 5.14 (d, 1H, C3'-H), 5.39 (d, 1H, C2'-H), 6.10 (s, 1H, C1'-H), 6.38 (s, 2H, NH₂), 6.96 (t, 1H, indole), 7.15 (t, 1H, -indole), 7.21 (s, 1H, indole), 7.32 (d, 1H, indole), 7.40 (t, 1H, -NH), 7.48 (d, 1H, indole), 7.80 (s, 1H, C8-H), 10.65 (s, 1H, N1-H), 10.78 (s, 1H, NH-indole) ppm [OHs exchanging with H₂O in NMR solvent].

Results

Operon structure of genes associated with *hinT*

In *E. coli* K-12 strains, the *hinT* gene is located adjacent to *yefL*, *yefM*, *yefN(thiK)*, *yefO(nagZ)*, and *yefP*. PCR analyses were performed to determine if the deletion/insertion mutations occurred in frame without affecting the operon structure. Results in Figure S1 show that the operon structure is still intact after deletion of each gene and insertion of a *kan* resistant gene. Further evidence of *hinT* deletion was obtained by measuring the phosphoramidase activity in cell-free lysates. Figure S2 shows that the *hinT* deletion mutant ($\Delta hinT$) did not have appreciable phosphoramidase activity that is

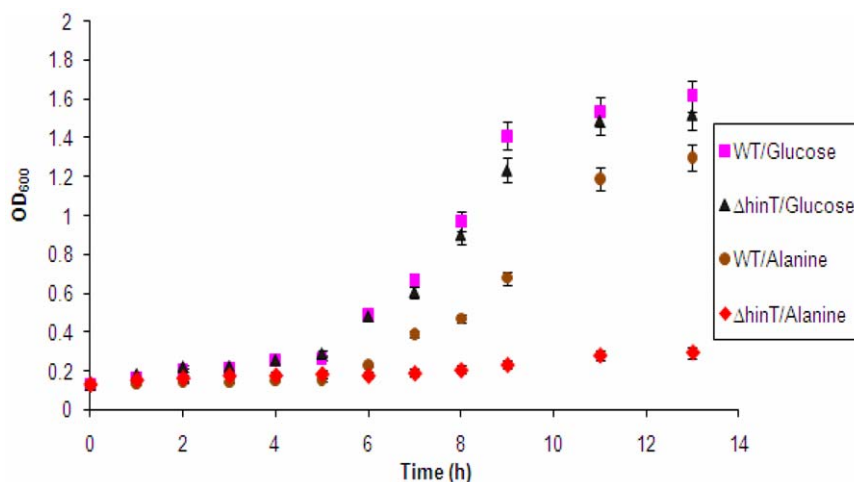


Figure 2. Bacterial growth curves of wild-type *E. coli* BW25113 and $\Delta hinT$ mutant in M9 medium in the presence of either 20 mM glucose or D,L-alanine. Measurements were done in duplicate and variants were less than 5% between two independent cultures. doi:10.1371/journal.pone.0020897.g002

associated with the expression of *hinT* in wild-type *E. coli* BW25113.

Phenotype of *ecHinT*

To ascertain the role of *ecHinT* in microbial metabolism, we obtained a series of mutants from the Keio collection containing deletions in the *hinT* (*ycfF*), *ycfL*, *ycfM*, *ycfN* (*thiK*), *ycfO* (*nagZ*), and *ycfP* genes. BiologTM plates were used for phenotypic screening to estimate the differential metabolic potential between wild-type *E. coli* BW25113 and the *hinT* deletion mutant (Δ *hinT*). Results from BiologTM substrate utilization studies (Fig. 1) indicated that metabolic profiles of wild-type *E. coli* BW25113 and the Δ *hinT* mutant were highly similar, with the exception of the utilization of D- and L-alanine. The initial screening results were verified and confirmed by culturing wild-type and mutant strains in minimal media containing D,L-alanine (Fig. 2). These results were highly reproducible, even when a starvation phase was introduced prior to culturing.

To further define the role of genes in the apparent *hinT* operon in alanine metabolism, *E. coli* strains from the Keio collection with verified deletions in *ycfL* (JW1090), *ycfM* (JW5157), *ycfN* (JW1092), *ycfO* (JW1093), and *ycfP* (JW5158) were evaluated for carbon source utilization. Compared to the wild-type BW25113 strain, none of the tested mutants showed significant differences in their ability to catabolize alanine when tested using BiologTM plates and test tube cultures (data not shown).

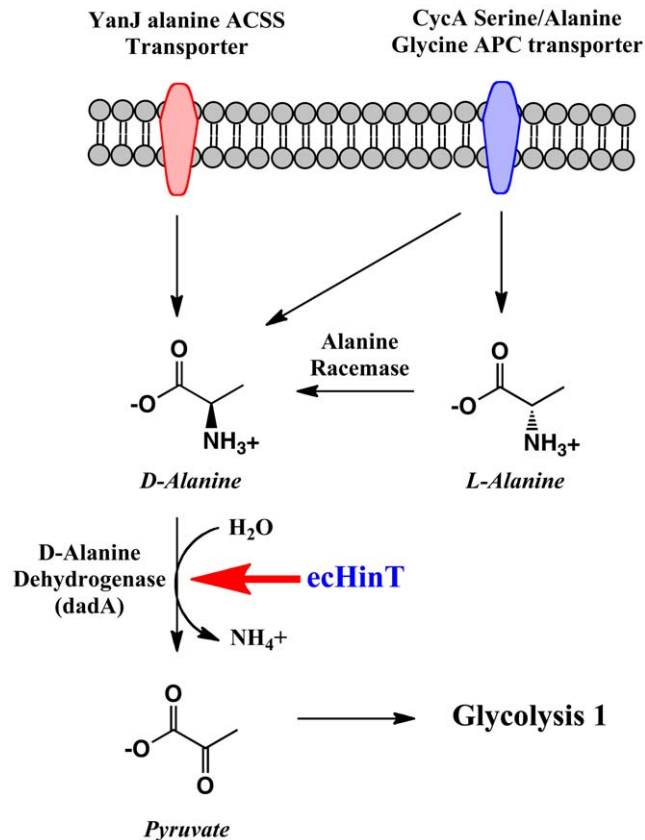


Figure 3. Alanine transport and metabolism in *E. coli* and the proposed role of *ecHinT*.

doi:10.1371/journal.pone.0020897.g003

D-amino acid transcription and activity testing

Inspection of the metabolic fingerprints of wild-type BW25113 and the Δ *hinT* mutant revealed that while the Δ *hinT* mutant failed to grow on both D and L isomers of alanine, it did grow on serine and glycine. Based on these results, and the known *E. coli* alanine catabolic pathway, we hypothesized that the Δ *hinT* mutant was neither deficient in the amino acid transporter system for D,L-alanine, nor in alanine racemase, but most likely in D-amino acid dehydrogenase activity encoded by *dadA* (Fig. 3). The inability of the Δ *hinT* mutant to grow on D,L-alanine can be explained by either failure to induce transcription of the D-amino-acid dehydrogenase or the presence of a defective D-amino-acid dehydrogenase that is incapable of metabolizing D-alanine. To test these hypotheses, RT-PCR was performed using primers for *dadA* and equivalent amounts of mRNA obtained from wild-type BW25113 or the Δ *hinT* mutant grown in the presence of D,L-alanine. Results in Figure 4 show that equivalent amounts of *dadA* transcript were produced by either the wild-type strain or the Δ *hinT* mutant. To determine if the inability of the Δ *hinT* mutant to grow on D-alanine was due to a lack of DadA enzyme activity, membrane fractions were isolated and analyzed for D-amino acid dehydrogenase activity. Results showed that the Δ *hinT* mutant possessed 38-fold less D-amino acid dehydrogenase activity (<5 nmol/min/mg) relative to the wild-type BW25113 strain (190 nmol/min/mg).

Phenotype rescue by *ecHinT*

Transformation of a plasmid encoding the wild-type *hinT* into the Δ *hinT* mutant (JW1089) allowed for growth on D,L-alanine to a level comparable to wild-type BW25113 grown under the same conditions (Fig. 5). This indicated that other mutations in strain JW1089 were not involved in the inability of the Δ *hinT* mutant to grow on D,L-alanine and that *hinT* was solely responsible for the observed phenotype.

A mutational approach was used to fully examine the relationship between *ecHinT* structure and activity, and DadA activity. Two active-site mutants were prepared and characterized as described previously [26]. The *ecHinT* H101 residue, which was previously shown to be required for enzymatic activity [26], was exchanged by site-directed mutagenesis into either alanine

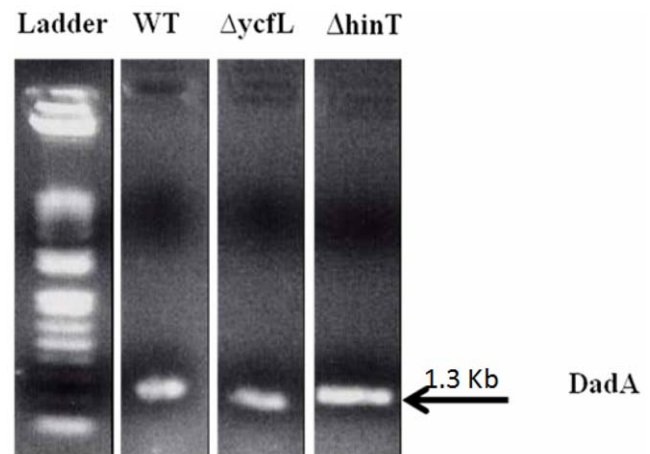


Figure 4. RT-PCR was performed with equivalent amounts of mRNA (100 ng) obtained from wild-type *E. coli* BW25113, Δ *hinT*, and Δ *ycfL* mutants using *dadA* primers under the described conditions. 1 μ g of each PCR reaction was loaded on 1% agarose gel.

doi:10.1371/journal.pone.0020897.g004

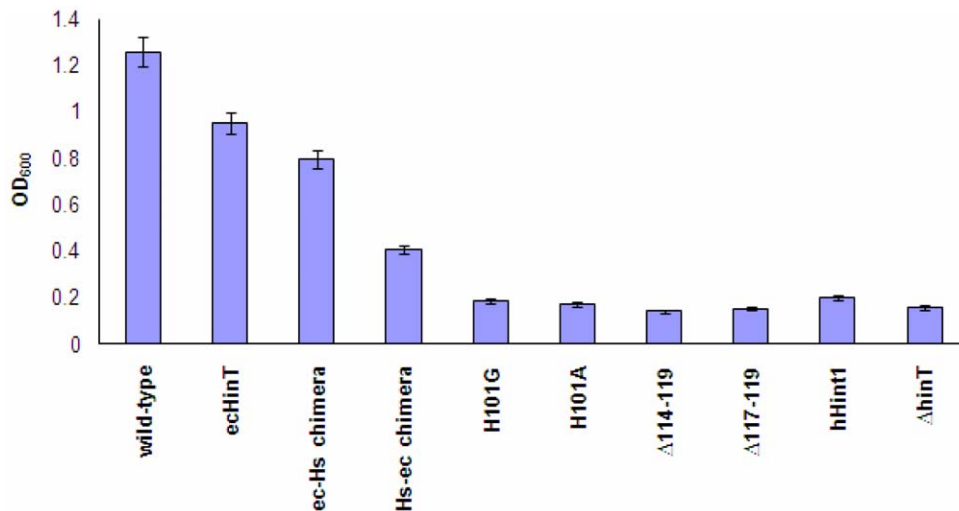


Figure 5. ecHinT structural and activity requirement for phenotype rescue. Each column represents the growth of the $\Delta hinT$ mutant that was transformed with a plasmid containing either *hintT*, a mutant *hinT*, *ec/Hs* chimera, *Hs/ec* chimera, or *hHint1*, except for the first column of wild-type *E. coli* BW25113. OD₆₀₀ values were determined 48 h after inoculation into M9 medium in presence of 20 mM D,L-alanine. doi:10.1371/journal.pone.0020897.g005

(H101A) or glycine (H101G). Enzymatic activity of these mutants were previously quantified by ³¹P-NMR using adenosine-5'-monophosphoramidate (AMP-NH₂) as a substrate and the catalytic efficiency was found to be approximately 30,000-fold lower than that of wild-type ecHinT [26]. Plasmids encoding the catalytically impaired mutants of ecHinT, H101A or H101G, failed to complement the $\Delta hinT$ mutant for growth on D,L-alanine. This indicated that catalytically active ecHinT is necessary for DadA activity (Fig. 5).

Remote deletion mutations that reside in the C-terminus region of ecHinT have been prepared and characterized previously [17]. The Michaelis-Menten parameters for the deletion mutants, $\Delta 114-119$ and $\Delta 117-119$, have been shown to be within an order of magnitude of the values for wild-type ecHinT. However, phenotype rescue was not observed after over-expressing these proteins in $\Delta hinT$ mutant strain (Fig. 5).

Design, synthesis and characterization of ecHinT inhibitor

Tryptamine guanosine carbamate (TpGc) was prepared according to synthetic Scheme S1. The rationale for designing such an inhibitor was based on the structural activity relationship of Hint substrates that were reported previously [23]. The phosphoramidate substrate tryptamine 5'-guanosine monophosphate (TpGd) (Fig. 6A) was found to be an excellent substrate with a k_{cat} value of 4.0 s⁻¹ and a k_{cat}/K_m value of 7.0×10^5 M⁻¹s⁻¹ [23]. It was hypothesized that substitution of the hydrolyzable phosphoramidate moiety with a carbamate linker (TpGc) would result in an inhibitor of ecHinT and not a substrate (Fig. 6B). In addition, the incorporation of guanosine would insure that off-target inhibition of Tryptophan tRNA synthetase would be minimized.

Using the previously described spectrophotometric phosphoramidase assay [23], the ecHinT K_i value for TpGc was determined. Although designed to be a competitive inhibitor, TpGc was found to exhibit apparent non-competitive inhibition of ecHinT with a K_i value of 42 μ M (Fig. 6C). Consistent with our previous finding, that ecHinT catalytic activity is required for the phenotype, when compared to the growth of $\Delta hinT$ *E. coli* strain on D,L-alanine, cultures of wild-type BW25113 grown in the

presence of D,L-alanine and 100 μ M of TpGc exhibited a similarly diminished growth capacity (Fig. 6D).

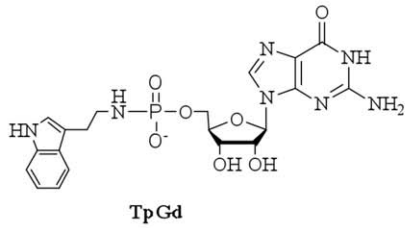
Discussion

The inducible *dadA* codes for the broad specificity bacterial D-amino-acid dehydrogenase. DadA catalyses the oxidation of D-amino acids, including alanine, into their corresponding ketoacids [27]. The bacterial D-amino-acid dehydrogenase is a heterodimer complex formed by a 45- and a 55-kDa subunit [28]. To avoid overproduction of reactive oxygen species that could damage cellular components, D-amino acid oxidation in bacteria is not coupled to O₂ reduction and the two electrons from the substrate are received by FAD in the small subunit before being transferred to a sulfur-iron center in the large subunit [28]. Bacterial D-amino-acid dehydrogenase appears to have two main functions in bacteria. Initially, it permits the growth of bacteria when D-amino acids are the sole carbon, nitrogen, and energy source [29,30]. Second, it prevents the accumulation of D-amino acids in cellular compartments, as some D-amino acid analogues have specific inhibitory effects on bacterial growth [31,32]. In bacteria, D-amino acids are used to stabilize the peptidoglycan structure [33], and have recently been shown to regulate biofilm disorganization [34], as well as play a role in quorum sensing.

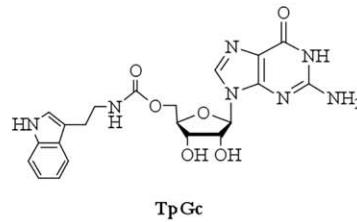
In this study, we report the first evidence of a regulatory relationship between the evolutionary conserved enzymes, DadA and ecHinT. Since transcripts encoding for *dadA* were produced in the $\Delta hinT$ mutant, our results suggested that D-amino acid dehydrogenase activity in *E. coli* is likely modulated by the interaction of ecHinT and DadA in a post-translational manner.

To probe structural elements of ecHinT that are determinant for the discovered phenotype, non-active-site deletion mutations that reside in the C-terminus region of ecHinT were prepared and characterized as described previously [17]. Recently, we investigated the C-terminal region of the ecHinT protein and found that this loop accommodates several conformational forms in the 1.3 \AA crystal structure (Fig. 7) [17]. We designed, and fully characterized, two deletion mutants of the ecHinT C-terminus in which three or six amino acids were deleted from the 11 amino acid

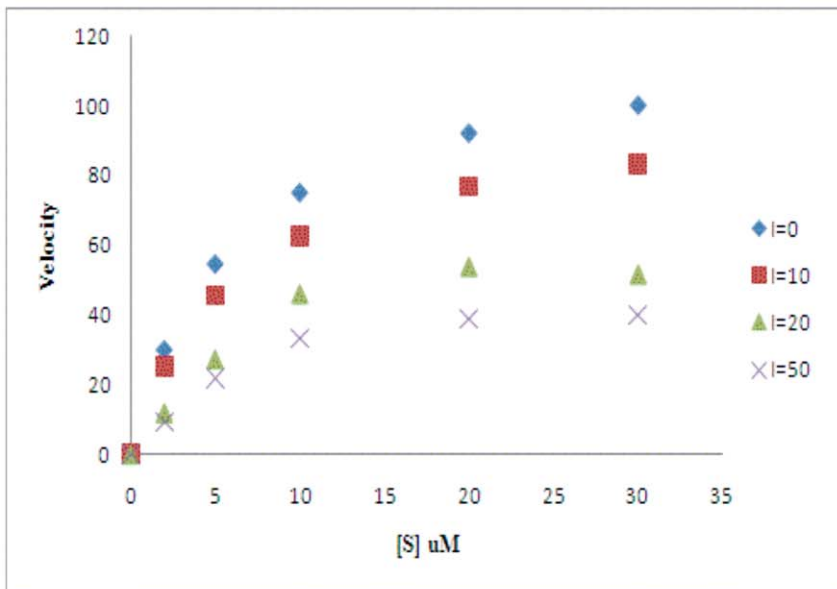
A)



B)



C)



D)

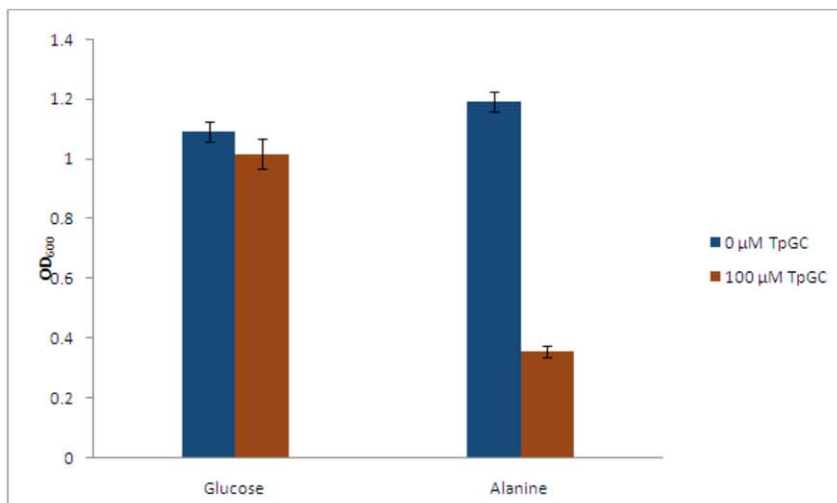


Figure 6. Inhibition of phenotype rescue by eHINT inhibitor. A) The structure of tryptamine 5'-guanosine monophosphate (TpGd). B) The structure of tryptamine guanosine carbamate (TpGc). C) TpGc exhibits a non-competitive inhibition profile. D) Wild-type *E. coli* BW25113 was grown in M9 medium supplemented with either 20 mM glucose or 20 mM alanine in the presence (brown bar) or absence (blue bar) of 100 μ M TpGC. OD₆₀₀ values were determined after 48 h. doi:10.1371/journal.pone.0020897.g006

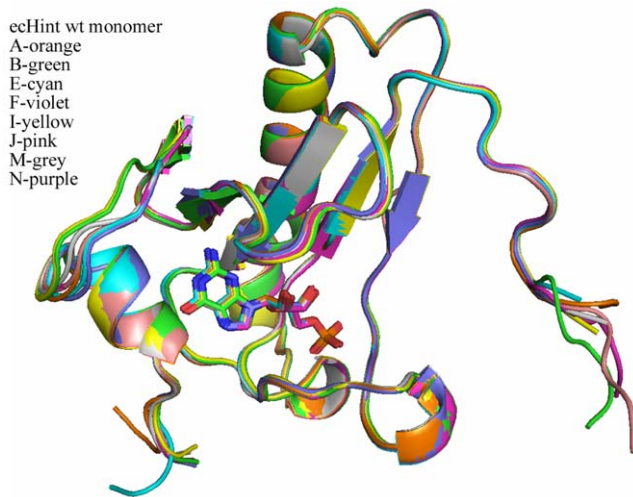


Figure 7. Superposition of the eight independent monomers observed in the structure of the wild-type ecHinT-GMP complex.

doi:10.1371/journal.pone.0020897.g007

C-terminal loop. The two deletion mutants were equivalent in their secondary structure to wild-type ecHinT and preserved the ability to form homodimers. The catalytic efficiencies of the deletion mutants were within one order of magnitude of the value determined for wild-type ecHinT. Despite the partial activity possessed by these mutants, both mutants failed to rescue *ΔhinT* growth on D,L-alanine.

Although both the N and C-terminal loops of ecHinT can adopt more than one conformation in the ecHinT-GMP complex structure [17], the overall fold of the structure is similar to hHint1 [17]. To investigate the possibility of phenotype rescue by hHint1, which is 48% homologous to ecHinT, the *E. coli ΔhinT* mutant was transformed with a plasmid encoding *hHint1* and the ability to grow on D,L-alanine examined. hHint1 failed to rescue the growth phenotype suggesting that certain structural characteristics, in addition to catalytic activity, govern the regulation of DadA activity by ecHinT. Based on our finding that the C-terminal loop of ecHinT plays a significant role in the observed relationship between ecHinT and DadA activity, the ability of two chimeric proteins to rescue *ΔhinT* cells was studied. The hHint1-ecHinT chimera (Hs/ec), in which the C-terminus of hHint1 was replaced with the ecHinT C-terminus, was unable to rescue the D-alanine growth defect exhibited by *E. coli ΔhinT* cells. In contrast, the ecHinT-hHint1 chimera (ec/Hs), in which the C-terminus of ecHinT was replaced with the hHint1 C-terminus, had only a slightly reduced ability to complement the phenotype when compared to wild-type ecHinT (Fig. 5).

Taken together, these results suggest that other inherent structural requirements, in addition to the C-terminus, are critical

References

- Brenner C, Bieganski P, Pace H, Huebner K (1999) The histidine triad superfamily of nucleotide-binding proteins. *J Cell Physiol* 181: 179–187.
- Brenner C (2002) Hint, Fhit, and GalT: function, structure, evolution, and mechanism of three branches of the histidine triad superfamily of nucleotide hydrolases and transferases. *Biochemistry* 41: 9003–9014.
- Korsisaari N, Makela TP (2000) Interactions of Cdk7 and Kin28 with Hint/PKCI-1 and Hnt1 histidine triad proteins. *J Biol Chem* 275: 34837–34840.
- Korsisaari N, Rossi DJ, Luukko K, Huebner K, Henkemeyer M, et al. (2003) The histidine triad protein Hint is not required for murine development or Cdk7 function. *Mol Cell Biol* 23: 3929–3935.
- Weiske J, Huber O (2005) The histidine triad protein Hint1 interacts with Pontin and Reptin and inhibits TCF-beta-catenin-mediated transcription. *J Cell Sci* 118: 3117–3129.
- Li H, Zhang Y, Su T, Santella RM, Weinstein IB (2006) Hint1 is a haplo-insufficient tumor suppressor in mice. *Oncogene* 25: 713–721.
- Yuan BZ, Jefferson AM, Popescu NC, Reynolds SH (2004) Aberrant gene expression in human non small cell lung carcinoma cells exposed to demethylating agent 5-aza-2'-deoxycytidine. *Neoplasia* 6: 412–429.
- Hsieh SY, Hsu CY, He JR, Liu CL, Lo SJ, et al. (2009) Identifying apoptosis-evasion proteins/pathways in human hepatoma cells via induction of cellular hormesis by UV irradiation. *J Proteome Res* 8: 3977–3986.

to the ecHinT-mediated DadA activation. Ongoing studies should shed light on the post-translational regulatory relationship between ecHinT and DadA and whether this regulation influences the localization, dimerization and/or degradation of DadA.

In summary, by using a series of mutagenic and chemical biological studies, ecHinT has been shown to be necessary for the growth of *E. coli* on D-alanine by regulating the catalytic activity of a key metabolizing enzyme, DadA. The role of ecHinT has been shown to be dependent on; the catalytic activity of ecHinT, components of its C-terminus domain and potentially unidentified structural factors. This marks only the second example of a direct relationship between the catalytic activity of a Hint protein and a physiological function [15]. Interestingly, the characteristics of ecHinT that appear necessary for the discovered phenotype are also required for the hydrolysis of LysU-generated lysyl-AMP by ecHinT [11,17]. Whether this observation is a coincidence or evidence of a catalytic link between the interaction of ecHinT with LysRS and DadA remains to be determined.

Supporting Information

Figure S1 Sequence verification PCR (representative gel). Forward primers were designed based on 5' end of the gene of interest and the reverse primers were designed based on junction point between *Kan* resistance gene and the following gene in the operon. The length of each obtained product equals the size of the gene of interest plus the size of *Kan* resistance gene. (DOC)

Figure S2 Progress curves for ecHinT phosphoramidase activity in *E. coli* wild-type (WT) and *ΔhinT* cell-free lysates. (DOC)

Table S1 Bacterial strains used in this study. (DOC)

Table S2 Primers used for sequence verification PCR reaction. (DOC)

Scheme S1 General synthetic scheme for TpGc. (DOC)

Acknowledgments

We thank Dr. Masayuki Sugawara for his help in conducting the Biolog screening experiments and for his helpful discussions.

Author Contributions

Conceived and designed the experiments: SB MS CRW. Performed the experiments: SB BG TFC. Analyzed the data: SB BG TFC MS CRW. Wrote the paper: SB MS CRW.

9. Martin J, Romanque P, Maurhofer O, Schmitter K, Ferrand G, et al. (2011) Ablation of the tumor suppressor histidine triad nucleotide binding protein 1 is protective against hepatic ischemia/reperfusion injury. *Hepatology* 53: 243–52.
10. Su T, Suzui M, Wang L, Lin CS, Xing WQ, et al. (2003) Deletion of histidine triad nucleotide-binding protein 1/PKC-interacting protein in mice enhances cell growth and carcinogenesis. *Proc Natl Acad Sci USA* 100: 7824–7829.
11. Chou T-F, Wagner CR (2007) Lysyl-tRNA synthetase-generated lysyl-adenylate is a substrate for histidine triad nucleotide binding proteins. *J Biol Chem* 282: 4719–4727.
12. Butland G, Peregrin-Alvarez JM, Li J, Yang W, Yang X, et al. (2005) Interaction network containing conserved and essential protein complexes in *Escherichia coli*. *Nature* 433: 531–537.
13. Hopfe M, Hoffmann R, Henrich B (2004) P80, the HinT interacting membrane protein, is a secreted antigen of *Mycoplasma hominis*. *BMC Microbiol* 4: 46.
14. Kitzrow A, Henrich B (2001) The cytosolic HinT protein of *Mycoplasma hominis* interacts with two membrane proteins. *Mol Microbiol* 41: 279–287.
15. Bieganowski P, Garrison PN, Hodawadekar SC, Faye G, Barnes LD, et al. (2002) Adenosine monophosphoramidase activity of Hint and Hnt1 supports function of Kin28, Ccl1, and Tib3. *J Biol Chem* 277: 10852–10860.
16. Lima CD, Klein MG, Weinstein IB, Hendrickson WA (1996) Three-dimensional structure of human protein kinase C interacting protein 1, a member of the HIT family of proteins. *Proc Natl Acad Sci USA* 93: 5357–5362.
17. Bardawel S, Pace J, Chou T-F, Cody V, Wagner CR (2010) Probing the impact of the *echinT* C-terminal domain on structure and catalysis. *J Mol Biol* 404: 627–638.
18. Chou T-F, Sham Y, Wagner CR (2007) Impact of the C-terminal loop of histidine triad nucleotide binding protein1 (Hint1) on substrate specificity. *Biochemistry* 46: 13074–13079.
19. Ito M, Baba T, Morib H, Mori H (2005) Functional analysis of 1440 *Escherichia coli* genes using the combination of knock-out library and phenotype microarrays. *Metab Engineering* 7: 318–327.
20. Baba T, Aral T, Hasegawa M, Takail Y, Okumural Y, et al. (2006) Construction of *Escherichia coli* K-12 in-frame, single-gene knock-out mutants: the Keio collection. *Mol Systems Biol* 2: 1–11.
21. Bochner BR, Gadzinski P, Panomitos E (2001) Phenotype microarrays for high-throughput phenotypic testing and assay of gene function. *Genome Res* 11: 1246–1255.
22. Sambrook J, Fritsch EF, Maniatis T (1989) *Molecular Cloning: a laboratory manual*. 2nd ed. N.Y., Cold Spring Harbor Laboratory Cold Spring Harbor Laboratory Press. pp 1659. ISBN 0-87969-309-6.
23. Chou T-F, Baraniak J, Kaczmarek R, Zhou X, Cheng J, et al. (2007) Phosphoramidate pronucleotides: A comparison of the phosphoramidase substrate specificity of human and *E. coli* histidine triad nucleotide binding proteins (Hint1). *Mol Pharmacol* 4: 208–217.
24. Franklin F, Venables W (1976) Biochemical, genetic, and regulatory studies of alanine catabolism in *Escherichia coli* K12. *Mol Gen Genet* 149: 229–237.
25. Abrahamson J, Baker L, Stephenson J, Wood J (1983) Proline Dehydrogenase from *Escherichia coli* K12, properties of the membrane associated enzyme. *Eur J Biochem* 134: 77–82.
26. Chou T-F, Bieganowski P, Shilinski K, Cheng J, Brenner C, et al. (2005) ³¹P NMR and genetic analysis establish hinT as the only *Escherichia coli* purine nucleoside phosphoramidase and as essential for growth under high salt conditions. *J Bio Chem* 280: 15356–15361.
27. Olsiewski PJ, Kaczorowski GJ, Walsh C (1980) Purification and properties of D-amino acid dehydrogenase, an inducible membrane-bound iron-sulfur flavoenzyme from *Escherichia coli*. *J Biol Chem* 255: 4487–4494.
28. Pollegioni L, Piubelli L, Sacchi S, Pilone MS, Molla G (2007) Physiological functions of D-amino acid oxidases: from yeast to humans. *Cell Mol Life Sci* 64: 1373–1394.
29. Raunio RP, Jenkins WT (1973) D-alanine oxidase from *Escherichia coli*: localization and induction by L-alanine. *J Bacteriol* 115: 560–566.
30. Deutch CE (2004) Oxidation of 3,4-dehydro-D-proline and other D-amino acid analogues by D-alanine dehydrogenase from *Escherichia coli*. *FEMS Microbiol Lett* 238: 383–389.
31. Lobočka M, Hennig J, Wild J, Klopotowski T (1994) Organization and expression of the *Escherichia coli* K-12 dad operon encoding the smaller subunit of D-amino acid dehydrogenase and the catabolic alanine racemase. *J Bacteriol* 176: 1500–1510.
32. Yasuda Y, Tochikubo K (1985) Germination-initiation and inhibitory activities of L- and D-alanine analogues for *Bacillus subtilis* spores. Modification of methyl group of L and D-alanine. *Microbiol Immunol* 29: 229–241.
33. Walsh CT (1989) Enzymes in the D-alanine branch of bacterial cell wall peptidoglycan assembly. *J Biol Chem* 264: 2393–2396.
34. Kolodkin-Gal I, Romero D, Cao S, Clardy J, Kolter R, et al. (2010) D-Amino Acids Trigger Biofilm Disassembly. *Science* 328: 627–629.